in vivo *38*: 640-646 (2024)
doi:10.21873/invivo.13483

Immunophenotypes and Tumor Immune Microenvironment in Hepatocellular Carcinoma With Macrotrabecular Massive and Vessels Encapsulating Tumor Clusters

JUN AKIBA[1], MASAMICHI NAKAYAMA[2], REIICHIRO KONDO[2], HIRONORI KUSANO[2], SACHIKO OGASAWARA[2], YUTARO MIHARA[2], MASAHIKO TANIGAWA[2], KANA TSUTSUI[2], YUTA YANO[2], DAIKI MIYAZAKI[2], SAEKO TOKISAWA[2], TOSHIYUKI MITSUHASHI[2], HIDETOSHI NOMURA[2], SAKIKO SANADA[2], HISAMUNE SAKAI[3], TORU HISAKA[3] and HIROHISA YANO[2]

[1]*Department of Diagnostic Pathology, Kurume University Hospital, Kurume, Japan;*
[2]*Department of Pathology, Kurume University School of Medicine, Kurume, Japan;*
[3]*Department of Surgery, Kurume University School of Medicine, Kurume, Japan*

Abstract. *Background/Aim: Recently, vessels encapsulating tumor clusters (VETC) pattern and macrotrabecular massive (MTM) pattern of hepatocellular carcinoma (HCC) have been reported as aggressive histological types. These histological patterns showed an immunosuppressive tumor immune microenvironment (TIME). Since there have been no reports on the differences of these two subtypes simultaneously, this study examined the immunophenotypes and TIME of MTM-HCC and VETC-HCC immunohistochemically. Patients and Methods: Seventy-four cases of previously diagnosed HCC, including 32 MTM-HCCs, 21 VETC-HCCs, and 21 conventional HCCs, were enrolled in immunohistochemical analysis. We conducted immunohistochemical analysis. Results: We found that MTM-HCC showed less frequent expression of HepPar-1, which is one of the most common hepatocytic markers. In MTM-HCC, the frequency of high expression levels of Keratin19, carbonic anhydrase (CA) IX, and PD-L1 was higher compared to VETC-HCC and conventional HCC. PD-L1 expression was found in 34.4% of MTM-HCC, 0% of VETC-HCC, and 19.0% of conventional HCC. The rate of PD-L1 expression in MTM-HCC was significantly higher than the others (p=0.0015). PD-L1 expression was significantly associated with epithelial cell adhesion molecules and CA IX expression, which are representative markers of tumor stemness and hypoxic conditions, respectively. The CD8 infiltration in VETC-HCC was significantly lower than that in conventional HCC. Conclusion: MTM-HCC had different immunophenotypes and TIMEs compared to HCC with the VETC pattern. Although both had immunosuppressive TIME, the elements forming TIME were quite different. To enhance the immune checkpoint inhibitor efficacy, changing TIME from a suppressive to an active form is essential.*

Correspondence to: Jun Akiba, Department of Diagnostic Pathology, Kurume University Hospital, Asahi-machi 67, Kurume, Japan. Tel/Fax: +81 942317651, e-mail: akiba@med.kurume-u.ac.jp

Key Words: Macrotrabecular hepatocellular carcinoma, vessels encapsulating tumor clusters hepatocellular carcinoma, immunophenotypes, tumor immune microenvironment.

Primary liver cancer was the sixth most common cancer and the third leading cause of cancer-related death worldwide in 2020 (1). Liver cancer remains a global health challenge and its incidence is growing worldwide. It is estimated that more than one million individuals will be affected by liver cancer annually by 2025 (2, 3).

In patients with unresectable hepatocellular carcinoma (HCC), the combination therapy with atezolizumab and bevacizumab has become the first-line treatment regime for unresectable HCC because it has resulted in better overall and progression-free survival outcomes than sorafenib (4). The combination of immune-checkpoint inhibitors with anti-angiogenic antibodies or tyrosine kinase inhibitors can drive immune cell infiltration into 'cold' tumors, thereby converting them to 'hot' tumors and increasing response rates (5). To obtain optimal efficacies for these treatments, assessment of the tumor immune microenvironment (TIME) is required. In some solid tumors, such as lung, uterine cervical, breast, and head and neck cancers, the assessment of TIME is routinely conducted by immunohistochemical staining for programed death-1 (PD-1) or PD-L1 (6-9). However, in HCC, no assessments have been conducted for b-catenin mutated/activated HCC and non-viral

Table I. *Clinicopathological characteristics of 74 hepatocellular carcinomas (HCCs).*

	MTM pattern	VETC pattern	Conventional HCC	*p*-Value
Case number	32	21	21	
Age (median [range])	67 [40, 87]	70 [43, 82]	72 [54, 82]	**0.0431**
Sex: n: F/M (%)	6/26 (19/81)	4/17 (19/81)	4/17 (19/81)	0.9995
AFP (ng/ml) (median [range])	520 [2, 42067]	520 [1.8, 7564]	5.8 [2.3, 745]	**<0.001**
DCP (mAU/ml) (median [range])	2229 [23, 75000]	455.5 [16, 75000]	48 [11, 26705]	**0.0392**
Size (mm) (median [range])	45 [15, 150]	37 [16, 160]	24 [12, 63]	**<0.001**
Histological grade: n (%)				**<0.001**
Well differentiated	0 (0)	0 (0.0)	1 (0.0)	
Moderately differentiated	11 (34.4)	16 (76.2)	19 (42.9)	
Poorly differentiated	21 (65.6)	5 (23.1)	1 (57.1)	
Portal vein invasion: absent/present n (%)	2/32 (6.3/93.7)	2/19 (9.5/90.5)	8/13 (38.1/61.9)	**0.0054**
Venous invasion: absent/present n (%)	31/1 (96.9/3.1)	19/2 (90.5/9.5)	21/0 (100/0)	0.2762
Fibrosis in the background liver CH/LC	23/9 (71.9/28.1)	15/6 (71.4/28.6)	15/6 (71.4/28.6)	0.6304
Etiology HBV/HCV/NBNC	10/13/10 (30.3/39.4/30.3)*	6/7/8 (28.6/33.3/38.1)	4/11/6 (19.1/52.4/28.6)	0.7832

AFP: Alfa-fetoprotein; DCP: des-γ-carboxy prothrombin; MTM: macrotrabecular massive; VETC: vessels encapsulating tumor cluster; CH: chronic hepatitis; LC: liver cirrhosis; HBV: hepatitis B virus, HCV: hepatitis C virus; NBNC: non HBV and non HCV. *one case showed both HBV and HCV infections. Statistically significant *p*-values are shown in bold.

associated HCC is known to show resistance to immune check point inhibitors (9-11).

Recently, vessels encapsulating tumor clusters (VETC) pattern has been reported as a predictor of sorafenib benefit in patients with HCC (12) and is associated with unfavorable prognosis (12, 13). HCCs with the VETC pattern are often accompanied by the macrotrabecular massive (MTM) pattern, which is also known as an aggressive histological type (13, 14). We previously reported that HCCs with MTM pattern and VETC pattern had significant numbers of the VETC pattern and the MTM pattern, respectively (14). Moreover, these histological patterns showed high PD-L1 expression and immunosuppressive TIME (15, 16).

Due to their morphological characteristics, the VETC pattern and MTM pattern are easy to recognize. However, diagnosis of HCC is expected to be difficult with the limited samples obtained from biopsies. To obtain correct diagnoses, pathologists must be able to recognize the immunophenotype of these aggressive HCC subtypes.

Although MTM and VETC patterns were often observed within the same nodule (13, 14), there are no reports on the differences between these two subtypes simultaneously. We examined the immunophenotypes and TIME of HCC with the MTM pattern and VETC pattern immunohistochemically in this study.

Patients and Methods

Patients. Seventy-four cases of previously diagnosed HCC were enrolled in this study. All cases were resected at Kurume University Hospital between 2006 and 2015. We randomly selected 32 HCCs with the MTM pattern and 21 HCCs with the VETC pattern based on our previous study (14). Twenty-one conventional HCCs were randomly selected. Pathological assessment was conducted by two pathologists (JA and MN). Clinicopathological findings are shown in Table I. This study was conducted in accordance with the Declaration of Helsinki and was approved by the ethics committee of Kurume University (approval #19017).

Tissue preparation and pathological assessment. Liver specimens were fixed in 10% formalin and embedded in paraffin. We cut 4-μm consecutive sections and stained them with hematoxylin and eosin. When a tumor nodule consisted of plural histological grades, the highest grade was adopted. For pathological diagnosis, we followed the WHO classification (17). The MTM pattern and the VETC pattern were defined following previous reports (13, 14). We conducted IHC using TMA sections, following the procedure of our previous study. Each slide contained 22 cores. We punctured paraffin-embedded samples in two cores from each case. Briefly, in HCC with the MTM pattern, tumor cells proliferated with thick trabecula consisting of more than six cells. In HCC with the VETC pattern, the tumor was composed of small tumor clusters covered with endothelial cells that are easily detectable morphologically.

Immunohistochemical staining. IHC was performed using the following antibodies: HepPar-1 (OCH1E5, Agilent Technologies, Inc., Santa Clara, CA, USA), arginase-1 (Sigma-Aldrich, St. Louis, MO, USA), glypican-3 (GPC3) (clone 1G12, Nichirei Bioscience Inc., Tokyo, Japan), Keratin (K) 19 (clone RCK108, Dako; Agilent Technologies, Inc.), epithelial cell adhesion molecule (EpCAM, clone VU1D9, Cell Signaling Technology, Danvers, MA, USA), carbonic anhydrase (CA) IX (H-11, Santa Cruz Biotechnology, Dallas, TX, USA), PD-L1 (clone E1L3N, Cell Signaling Technology,), and CD8 (clone 4B11, Leica Biosystems, Newcastle, UK).

Table II. *The association between hepatocellular carcinoma (HCC) subtypes and hepatobiliary markers.*

Markers		MTM pattern	VETC pattern	Conventional HCC	*p*-Value
HepPar-1	[low/high: n (%)]	20/12 (62.5/37.5)	2/19 (9.5/90.5)	0/21 (0/100)	**<0.0001**
Arginase-1	[low/high: n (%)]	11/21 (34.4/65.6)	3/18 (14.3/85.7)	2/19 (9.5/90.5)	0.0623
Glypican-3	[low/high: n (%)]	27/5 (84.4/15.6)	16/5 (76.1/23.8)	18/3 (85.7/14.3)	0.6688
Keratin 19	[absent/present: n (%)]	28/4 (87.5/12.5)	21/0 (100/0)	21/0 (100/0)	**0.0301**
EpCAM	[absent/present: n (%)]	28/4 (87.5/12.5)	19/2 (90.5/9.5)	20/1 (95.4/4.6)	0.6419
CA IX	[low/high: n (%)]	20/12 (62.5/37.5)	21/0 (100/0)	16/5 (76.2/23.8)	**0.0064**
PD-L1	[absent/present: n (%)]	21/11 (65.6/34.4)	21/0 (100/0)	17/4 (81.0/19.0)	**0.0015**
CD8	cells/mm^2, median [range]	21 [0, 1062]	5 [0, 173]	33 [13, 2281]	**0.0424**

MTM: Macrotrabecular massive; VETC: vessels encapsulating tumor cluster; HepPar-1: hepatocyte paraffin-1; Epcam: epithelial cell adhesion molecule; CA IX: carbonic anhydrase IX; tPD-L1: tumor programed death-ligand 1; stromal programed death-ligand 1. Statistically significant *p*-values are shown in bold.

The expression of PD-L1 was evaluated in conjunction with tumoral and stromal expression. Based on previous reports, the cut-off value for PD-L1 expression was set as 1% (18, 19). CD8-positive tumor infiltrating lymphocytes were also evaluated. These cells were manually counted in five high-power fields of view (magnification: ×400) and the average number of cells per mm^2 was determined. Cut-off values were determined as >1% for K19 and EpCAM and were >50% for HepPar-1, arginase-1, GPC3, and CA IX. IHC staining for HepPar-1, K19, CD8, and PD-L1 was performed using BOND-III (Leica Microsystems, Newcastle, UK). IHC for the others was conducted using BenchMark ULTRA (Roche Diagnostics, Tucson, AZ, USA).

Statistical analysis. Intergroup differences in categorical variables and IHC results were examined using the Chi-square test or Fisher's exact test. Differences of $p<0.05$ were considered significant. All analyses were conducted using JMP version 16 software (SAS Institute Inc., Cary, NC, USA).

Results

Clinicopathological findings. Patients with HCC with the MTM pattern were significantly younger those of the others ($p=0.0431$). Tumor markers, such as α-fetoprotein (AFP) and des-γ-carboxy prothrombin (DCP), of the MTM pattern and VETC pattern were significantly higher than those of conventional HCC ($p<0.0001$ and $p=0.0392$, respectively). Tumor size of the MTM pattern and VETC pattern HCC was significantly larger than that of conventional HCC ($p<0.001$). HCC with the MTM pattern and VETC pattern showed significantly high histological grades ($p<0.001$) and high frequency of portal vein invasion ($p=0.0054$).

Immunohistochemical staining of HCCs. The results of IHC are summarized in Table II. The number of cases with HepPar-1 high expression in the MTM pattern was significantly lower than that in the VETC pattern and conventional HCC ($p<0.0001$). There were no significant differences among the three groups in arginase-1 expression although that expression in the MTM pattern tended to be lower compared to the others. K19 expression was found only in the MTM pattern and not found in the VETC pattern and conventional HCC ($p=0.0301$). The expression of CA IX and PD-L1 was found in the MTM pattern and conventional HCC and was not found in the VETC pattern ($p=0.0064$ and 0.0015, respectively). There were no significant differences in Glypican-3 and EpCAM expression among the groups. The VETC pattern of HCC exhibited a significantly lower CD8 infiltration compared to conventional HCC (Figure 1). No significant differences were found between the others.

Table III. *Correlation between PD-L1 expression and several hepatobiliary markers.*

Markers		PD-L1		*p*-Value
		Absent	Present	
HepPar-1	Low	14	8	**0.0305**
	High	45	7	
Arginase-1	Low	12	4	0.6019
	High	47	11	
Glypican-3	Low	53	8	0.3824
	High	10	3	
Keratin 19	Absent	57	13	0.1712
	Present	2	2	
EpCAM	Absent	56	11	**0.0224**
	Present	3	4	
CA IX	Low	50	7	**0.0033**
	High	9	8	

HepPar-1: Hepatocyte paraffin-1; EpCAM: epithelial cell adhesion molecule; CA IX: carbonic anhydrase IX; PD-L1: programed death-ligand 1. Statistically significant *p*-values are shown in bold.

Correlation between PD-L1 expression and several hepatobiliary markers. The results of correlation between PD-L1 expression in the tumor and stroma and hepatobiliary

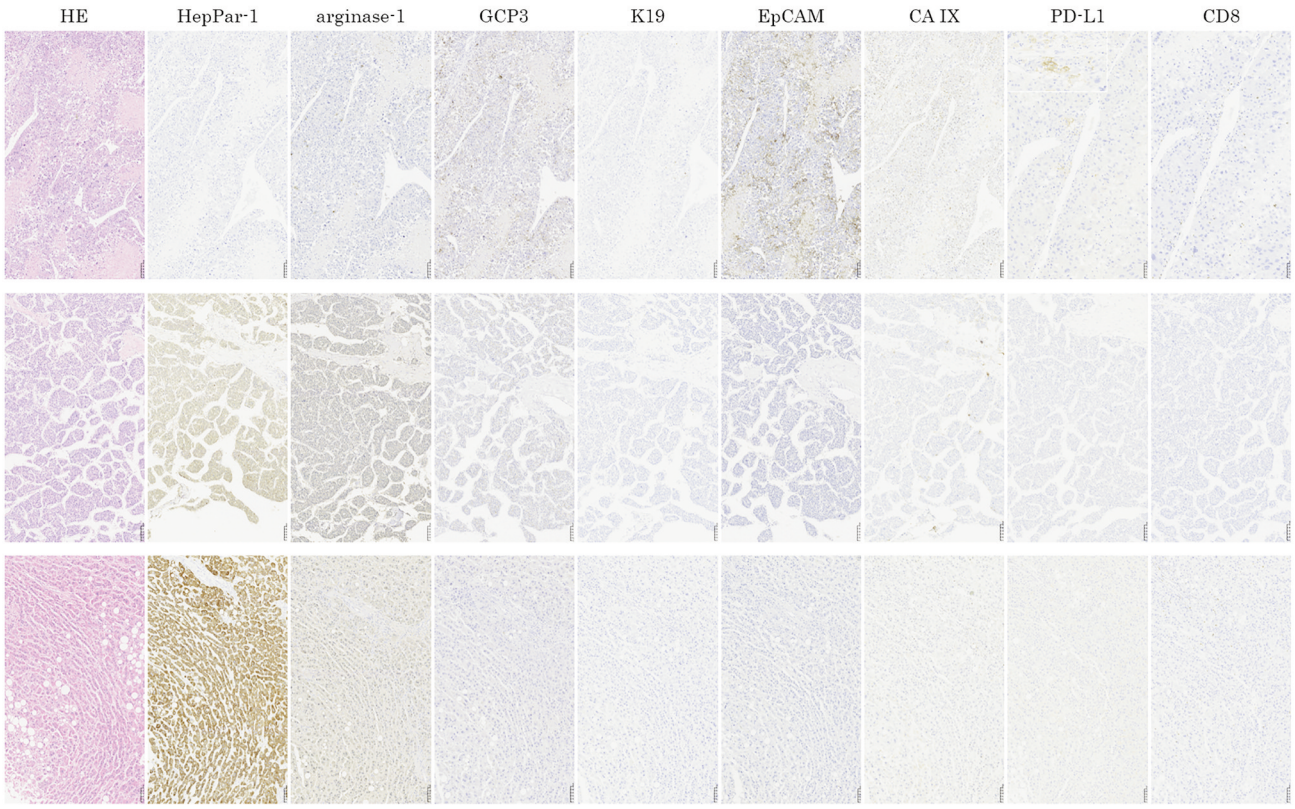

Figure 1. *Representative microphotographs of the hepatocellular carcinoma (HCC)-macrotrabecular massive pattern, HCC-vessels encapsulating tumor clusters pattern, and conventional HCC are shown in the upper, middle, and lower arrows, respectively. The microphotographs in the same row originate from the same case. Scale bar indicates 100 mm.*

markers are summarized in Table III. PD-L1 expression was significantly correlated with low HepPar-1, high EpCAM, and high CA IX expression (p=0.0305, p=0.0224, and p=0.0033, respectively).

Discussion

In this study, we found that HCC with the MTM pattern showed less frequent expression of HepPar-1, which is one of the most common hepatocytic markers. Moreover, in MTM-HCC, the frequency of high expressions of K19, CA IX, and PD-L1 was higher compared to VETC-HCC and conventional HCC. PD-L1 expression was associated with tumor stemness and hypoxic conditions. In addition, HCC with the MTM pattern and VETC pattern had different immunophenotypes and TIME.

Clinicopathological findings of HCC with the MTM pattern and VETC pattern are mostly comparable with our previous study (14). Briefly, HCC with the MTM pattern and VETC pattern demonstrated aggressive features, such as high levels of tumor markers, large tumor size, less differentiation, and frequent portal vein invasion. Although this cohort was composed of a small number of cases, the accompanying biological characteristics of these subtypes were similar with previous reports (12-14).

In HCC with the MTM pattern, the representative hepatocytic marker HepPar-1 showed significantly low expression and arginase-1 expression tended to be lower compared to HCC with the VETC pattern and conventional HCC. To date, there have been no reports on hepatocytic markers in HCC with the MTM pattern. However, these results are associated with the fact that HepPar-1 and arginase-1 expression are decreased with less differentiation (20) as most HCCs with the MTM pattern show poorly differentiated HCC. In surgical specimens, pathological diagnosis of HCC with the MTM pattern is easy. However, HCCs with the MTM pattern often showed different imaging patterns compared to conventional HCCs (21, 22). Therefore, these cases may undergo liver biopsy. When a characteristic trabecular component is not observed in a tiny sample, pathologists may be unsure of the diagnosis for HCCs and conduct IHC for hepatocytic markers as well as biliary markers. In this study, significant expression of K19, a representative biliary marker, was found only in HCC with

the MTM pattern. In this situation, pathologists should not misinterpret HCC with the MTM pattern as poorly differentiated cholangiocarcinoma. It is well known that a small subset of HCC has K19 expression and shows poor prognosis (23). In addition, the prevalence of CA IX expression was notably higher in HCC exhibiting the MTM pattern when compared to other subtypes, in line with findings from a prior study (24). CA IX is not specific to HCCs and its expression is observed in various carcinomas, inducing hypoxic conditions (25-28). In pathological diagnosis, morphological and immunophenotypic findings as well as high levels of tumor markers can be useful.

In this study, to examine TIME of the MTM pattern and the VETC pattern, we conducted IHC using TMA sections. The MTM pattern showed significantly high expression of PD-L1 in both tumor and stromal cells. PD-L1 expression was found in 34.4% of HCC with the MTM pattern. A previous study by Liu *et al*. reported that PD-L1 expression was found in 43% of HCC with the MTM pattern and this rate was significantly higher than that of the non-MTM pattern HCC (16). In our study, no HCCs with the VETC pattern expressed tumoral PD-L1. Itoh *et al*. reported that the VETC pattern was associated with a significantly high rate of tumoral PD-L1 positivity in HCC tissues (38.1%) compared with non-VETC (8.3%) (15). On the other hand, Kurebayashi *et al*. demonstrated that most HCCs-MTM and VETC patterns belonged to immune-low/angiogenic subtypes and the expression of PDCD1LG1 and PDCD1LG2, which encode interferon-g-inducible immune checkpoint molecules, PD-L1 and PD-L2, respectively, was also down-regulated in immune-low/angiogenic subtypes (29). This difference may be attributed to the different cohort and different analytical methods. However, the underlying causes are unknown. HCC with the MTM pattern and the VETC pattern could have different tumoral microenvironments. Regarding the correlation between PD-L1 expression and other hepatic markers, low HepPar-1 expression, high EpCAM expression, and high CA IX expression are significantly associated. Higher histological grade HCC is known to frequently demonstrate lower HepPar-1 expression and showed significantly higher PD-L1 expression (30). EpCAM is a representative biliary marker as well as a cancer stem cell (CSC)/hepatic progenitor marker in HCC. Also, CA IX is a sensitive biomarker of hypoxia. Hypoxia can enhance HCC stemness (31). Liver CSCs contribute to the evasion of immunosurveillance by altering the phenotype of dendritic cells and impairing their recruitment (32, 33). Subsequently, in cases with high expression of EpCAM and CA IX, it is presumed that elevated PD-L1 expression was induced to evade immune surveillance.

Study limitations. First, the sample size used in this study was small. Second, we conducted the immunohistochemical study using TMA sections. Although we revealed that the MTM pattern and VETC pattern had different immunophenotypes and TIME, we were unable to verify the heterogeneity of TIME within the same nodule. To solve these problems, research with a large-scale sample and whole slide sections should be conducted.

Conclusion

We demonstrated that HCC with the MTM pattern had different immunophenotypes and TIMEs compared to HCC with the VETC pattern. Although both of them had immunosuppressive TIME as shown in previous reports, the elements forming TIME were quite different. To enhance immune checkpoint inhibitor efficacy, changing TIME from suppressive type to active type is essential. Therefore, conducting combination therapy using atezolizumab and bevacizumab is suitable for HCC with the MTM pattern and VETC pattern.

Conflicts of Interest

The have no conflicts of interest to declare in relation to this study.

Authors' Contributions

JA designed this study and drafted the manuscript. JA, MN, RK, HK, and SO conducted immunohistochemical staining and assessed the results. JA, MN, YM, MT, KT, YY, and DK participated in pathological diagnosis. JA, ST, TM, and HN constructed tissue microarray sections. HS and TH acquired and collected the samples. SS and HY edited the manuscript.

Acknowledgements

The Authors would like to thank Ms. Akiko Tanaka for her excellent preparation of sections.

References

1 Sung H, Ferlay J, Siegel RL, Laversanne M, Soerjomataram I, Jemal A, Bray F: Global Cancer Statistics 2020: GLOBOCAN estimates of incidence and mortality worldwide for 36 cancers in 185 countries. CA Cancer J Clin 71(3): 209-249, 2021. DOI: 10.3322/caac.21660

2 Llovet JM, Zucman-Rossi J, Pikarsky E, Sangro B, Schwartz M, Sherman M, Gores G: Hepatocellular carcinoma. Nat Rev Dis Primers 2(1): 16018, 2016. DOI: 10.1038/nrdp.2016.18

3 Villanueva A: Hepatocellular carcinoma. N Engl J Med 380(15): 1450-1462, 2019. DOI: 10.1056/NEJMra1713263

4 Finn RS, Qin S, Ikeda M, Galle PR, Ducreux M, Kim TY, Kudo M, Breder V, Merle P, Kaseb AO, Li D, Verret W, Xu DZ, Hernandez S, Liu J, Huang C, Mulla S, Wang Y, Lim HY, Zhu AX, Cheng AL, IMbrave150 Investigators: Atezolizumab plus bevacizumab in unresectable hepatocellular carcinoma. N Engl J Med 382(20): 1894-1905, 2020. DOI: 10.1056/NEJMoa1915745

5 Llovet JM, Castet F, Heikenwalder M, Maini MK, Mazzaferro V, Pinato DJ, Pikarsky E, Zhu AX, Finn RS: Immunotherapies for hepatocellular carcinoma. Nat Rev Clin Oncol 19(3): 151-172, 2022. DOI: 10.1038/s41571-021-00573-2

6 Reck M, Rodríguez-Abreu D, Robinson AG, Hui R, Csőszi T, Fülöp A, Gottfried M, Peled N, Tafreshi A, Cuffe S, O'Brien M, Rao S, Hotta K, Leiby MA, Lubiniecki GM, Shentu Y, Rangwala R, Brahmer JR: Pembrolizumab *versus* chemotherapy for PD-L1-positive non–small-cell lung cancer. N Engl J Med 375(19): 1823-1833, 2016. DOI: 10.1056/NEJMoa1606774

7 Colombo N, Dubot C, Lorusso D, Caceres MV, Hasegawa K, Shapira-Frommer R, Tewari KS, Salman P, Hoyos Usta E, Yañez E, Gümüş M, Olivera Hurtado de Mendoza M, Samouëlian V, Castonguay V, Arkhipov A, Toker S, Li K, Keefe SM, Monk BJ: Pembrolizumab for persistent, recurrent, or metastatic cervical cancer. N Engl J Med 385(20): 1856-1867, 2021. DOI: 10.1056/NEJMoa2112435

8 Emens LA, Molinero L, Loi S, Rugo HS, Schneeweiss A, Diéras V, Iwata H, Barrios CH, Nechaeva M, Nguyen-Duc A, Chui SY, Husain A, Winer EP, Adams S, Schmid P: Atezolizumab and nab-paclitaxel in advanced triple-negative breast cancer: biomarker evaluation of the IMpassion130 study. J Natl Cancer Inst 113(8): 1005-1016, 2021. DOI: 10.1093/jnci/djab004

9 Burtness B, Harrington KJ, Greil R, Soulières D, Tahara M, de Castro G Jr, Psyrri A, Basté N, Neupane P, Bratland Å, Fuereder T, Hughes BGM, Mesía R, Ngamphaiboon N, Rordorf T, Wan Ishak WZ, Hong RL, González Mendoza R, Roy A, Zhang Y, Gumuscu B, Cheng JD, Jin F, Rischin D, KEYNOTE-048 Investigators: Pembrolizumab alone or with chemotherapy *versus* cetuximab with chemotherapy for recurrent or metastatic squamous cell carcinoma of the head and neck (keynote-048): A randomised, open-label, phase 3 study. Lancet 394(10212): 1915-1928, 2019. DOI: 10.1016/s0140-6736(19)32591-7

10 Cheng AL, Hsu C, Chan SL, Choo SP, Kudo M: Challenges of combination therapy with immune checkpoint inhibitors for hepatocellular carcinoma. J Hepatol 72(2): 307-319, 2020. DOI: 10.1016/j.jhep.2019.09.025

11 Harding JJ, Nandakumar S, Armenia J, Khalil DN, Albano M, Ly M, Shia J, Hechtman JF, Kundra R, El Dika I, Do RK, Sun Y, Kingham TP, D'Angelica MI, Berger MF, Hyman DM, Jarnagin W, Klimstra DS, Janjigian YY, Solit DB, Schultz N, Abou-Alfa GK: Prospective genotyping of hepatocellular carcinoma: Clinical implications of next-generation sequencing for matching patients to targeted and immune therapies. Clin Cancer Res 25(7): 2116-2126, 2019. DOI: 10.1158/1078-0432.CCR-18-2293

12 Fang JH, Xu L, Shang LR, Pan CZ, Ding J, Tang YQ, Liu H, Liu CX, Zheng JL, Zhang YJ, Zhou ZG, Xu J, Zheng L, Chen MS, Zhuang SM: Vessels that encapsulate tumor clusters (VETC) pattern is a predictor of sorafenib benefit in patients with hepatocellular carcinoma. Hepatology 70(3): 824-839, 2019. DOI: 10.1002/hep.30366

13 Renne SL, Woo HY, Allegra S, Rudini N, Yano H, Donadon M, Viganò L, Akiba J, Lee HS, Rhee H, Park YN, Roncalli M, Di Tommaso L: Vessels encapsulating tumor clusters (VETC) is a powerful predictor of aggressive hepatocellular carcinoma. Hepatology 71(1): 183-195, 2020. DOI: 10.1002/hep.30814

14 Akiba J, Nakayama M, Sadashima E, Kusano H, Kondo R, Mihara Y, Naito Y, Mizuochi S, Yano Y, Kinjo Y, Tsutsui K, Kondo K, Sakai H, Hisaka T, Nakashima O, Yano H: Prognostic impact of vessels encapsulating tumor clusters and macrotrabecular patterns in hepatocellular carcinoma. Pathol Res Pract 238: 154084, 2022. DOI: 10.1016/j.prp.2022.154084

15 Itoh S, Yoshizumi T, Yugawa K, Imai D, Yoshiya S, Takeishi K, Toshima T, Harada N, Ikegami T, Soejima Y, Kohashi K, Oda Y, Mori M: Impact of immune response on outcomes in hepatocellular carcinoma: Association with vascular formation. Hepatology 72(6): 1987-1999, 2020. DOI: 10.1002/hep.31206

16 Liu LL, Zhang SW, Chao X, Wang CH, Yang X, Zhang XK, Wen YL, Yun JP, Luo RZ: Coexpression of CMTM6 and PD-L1 as a predictor of poor prognosis in macrotrabecular-massive hepatocellular carcinoma. Cancer Immunol Immunother 70(2): 417-429, 2021. DOI: 10.1007/s00262-020-02691-9

17 WHO Classification of Tumours. 5th ed. Chapter 8, Tumours of the liver and intrahepatic bile ducts. Lyon, France, International Agency for Research on Cancer, 2019.

18 Kawaguchi A, Akiba J, Kondo R, Sadashima E, Ogasawara S, Naito Y, Kusano H, Sanada S, Muto I, Nakama T, Yano H: Programmed death-ligand 1 and programmed death-ligand 2 expression can affect prognosis in extramammary Paget's disease. Anticancer Res 41(1): 219-226, 2021. DOI: 10.21873/anticanres.14768

19 Sato F, Akiba J, Kawahara A, Naito Y, Ono T, Takase Y, Murata K, Abe H, Yamaguchi T, Miyoshi H, Abe Y, Mihara Y, Tanikawa M, Akashi M, Kurose H, Umeno H, Yano H: The expression of programed death ligand-1 could be related with unfavorable prognosis in salivary duct carcinoma. J Oral Pathol Med 47(7): 683-690, 2018. DOI: 10.1111/jop.12722

20 Timek DT, Shi J, Liu H, Lin F: Arginase-1, HepPar-1, and Glypican-3 are the most effective panel of markers in distinguishing hepatocellular carcinoma from metastatic tumor on fine-needle aspiration specimens. Am J Clin Pathol 138(2): 203-210, 2012. DOI: 10.1309/ajcpk1zc9wnhccmu

21 Rhee H, Cho ES, Nahm JH, Jang M, Chung YE, Baek SE, Lee S, Kim MJ, Park MS, Han DH, Choi JY, Park YN: Gadoxetic acid-enhanced MRI of macrotrabecular-massive hepatocellular carcinoma and its prognostic implications. J Hepatol 74(1): 109-121, 2021. DOI: 10.1016/j.jhep.2020.08.013

22 Cha H, Choi JY, Park YN, Han K, Jang M, Kim MJ, Park MS, Rhee H: Comparison of imaging findings of macrotrabecular-massive hepatocellular carcinoma using CT and gadoxetic acid–enhanced MRI. Eur Radiol 33(2): 1364-1377, 2022. DOI: 10.1007/s00330-022-09105-7

23 Govaere O, Komuta M, Berkers J, Spee B, Janssen C, de Luca F, Katoonizadeh A, Wouters J, van Kempen LC, Durnez A, Verslype C, De Kock J, Rogiers V, van Grunsven LA, Topal B, Pirenne J, Vankelecom H, Nevens F, van den Oord J, Pinzani M, Roskams T: Keratin 19: a key role player in the invasion of human hepatocellular carcinomas. Gut 63(4): 674-685, 2014. DOI: 10.1136/gutjnl-2012-304351

24 Calderaro J, Meunier L, Nguyen CT, Boubaya M, Caruso S, Luciani A, Amaddeo G, Regnault H, Nault JC, Cohen J, Oberti F, Michalak S, Bouattour M, Vilgrain V, Pageaux GP, Ramos J, Barget N, Guiu B, Paradis V, Aubé C, Laurent A, Pawlotsky JM, Ganne-Carrié N, Zucman-Rossi J, Seror O, Ziol M: ESM1 as a marker of macrotrabecular-massive hepatocellular carcinoma. Clin Cancer Res 25(19): 5859-5865, 2019. DOI: 10.1158/1078-0432.Ccr-19-0859

25 Kim K, Park WY, Kim JY, Sol MY, Shin DH, Park DY, Lee CH, Lee JH, Choi KU: Prognostic relevance of the expression of CA

IX, GLUT-1, and VEGF in ovarian epithelial cancers. Korean J Pathol 46(6): 532-540, 2012. DOI: 10.4132/KoreanJPathol.2012.46.6.532

26 McDonald PC, Chafe SC, Brown WS, Saberi S, Swayampakula M, Venkateswaran G, Nemirovsky O, Gillespie JA, Karasinska JM, Kalloger SE, Supuran CT, Schaeffer DF, Bashashati A, Shah SP, Topham JT, Yapp DT, Li J, Renouf DJ, Stanger BZ, Dedhar S: Regulation of pH by carbonic anhydrase 9 mediates survival of pancreatic cancer cells with activated KRAS in response to hypoxia. Gastroenterology 157(3): 823-837, 2019. DOI: 10.1053/j.gastro.2019.05.004

27 Sufian MA, Zamanova S, Shabana AM, Kemp B, Mondal UK, Supuran CT, Ilies MA: Expression dynamics of CA IX epitope in cancer cells under intermittent hypoxia correlates with extracellular pH drop and cell killing by ureido-sulfonamide CA IX inhibitors. Int J Mol Sci 24(5): 4595, 2023. DOI: 10.3390/ijms24054595

28 Haupt V, Gündel D, Prell E, Kahnt M, Sommerwerk S, Riemann A, Paschke R, Csuk R, Odparlik A, Thews O: Evaluation of betulinic acid derivatives as PET tracers for hypoxia-induced carbonic anhydrase IX (CA IX) expression. Adv Exp Med Biol 1395: 275-280, 2022. DOI: 10.1007/978-3-031-14190-4_45

29 Kurebayashi Y, Matsuda K, Ueno A, Tsujikawa H, Yamazaki K, Masugi Y, Kwa WT, Effendi K, Hasegawa Y, Yagi H, Abe Y, Kitago M, Ojima H, Sakamoto M: Immunovascular classification of HCC reflects reciprocal interaction between immune and angiogenic tumor microenvironments. Hepatology 75(5): 1139-1153, 2022. DOI: 10.1002/hep.32201

30 Jung HI, Jeong D, Ji S, Ahn TS, Bae SH, Chin S, Chung JC, Kim HC, Lee MS, Baek MJ: Overexpression of PD-L1 and PD-L2 is associated with poor prognosis in patients with hepatocellular carcinoma. Cancer Res Treat 49(1): 246-254, 2017. DOI: 10.4143/crt.2016.066

31 Cui CP, Wong CC, Kai AK, Ho DW, Lau EY, Tsui YM, Chan LK, Cheung TT, Chok KS, Chan ACY, Lo RC, Lee JM, Lee TK, Ng IOL: SENP1 promotes hypoxia-induced cancer stemness by HIF-1α deSUMOylation and SENP1/HIF-1α positive feedback loop. Gut 66(12): 2149-2159, 2017. DOI: 10.1136/gutjnl-2016-313264

32 Pardee AD, Shi J, Butterfield LH: Tumor-derived α-fetoprotein impairs the differentiation and T cell stimulatory activity of human dendritic cells. J Immunol 193(11): 5723-5732, 2014. DOI: 10.4049/jimmunol.1400725

33 Zhong M, Zhong C, Cui W, Wang G, Zheng G, Li L, Zhang J, Ren R, Gao H, Wang T, Li X, Che J, Gohda E: Induction of tolerogenic dendritic cells by activated TGF-β/Akt/Smad2 signaling in RIG-I-deficient stemness-high human liver cancer cells. BMC Cancer 19(1): 439, 2019. DOI: 10.1186/s12885-019-5670-9

Received November 15, 2023
Revised December 13, 2023
Accepted December 18, 2023